Bioorganic & Medicinal Chemistry Letters 22 (2012) 4094–4099

Contents lists available at SciVerse ScienceDirect

Bioorganic & Medicinal Chemistry Letters

journal homepage: www.elsevier.com/locate/bmcl

Ethyl 2,4,6-trihydroxybenzoate is an agonistic ligand for liver X receptor that induces cholesterol efflux from macrophages without affecting lipid accumulation in HepG2 cells

Minh-Hien Hoang [a], Yaoyao Jia [a], Hee-jin Jun [a], Ji-Hae Lee [a], Dong-Ho Lee [a], Bang-Yeon Hwang [b], Woo-Jin Kim [c], Hak-Ju Lee [c], Sung-Joon Lee [a,*]

[a] Department of Biotechnology, Graduate School of Life Sciences and Biotechnology, Korea University, Seoul 136-713, South Korea
[b] College of Pharmacy, Chungbuk National University, Cheongju, Chungbuk 361-763, Republic of Korea
[c] Division of Green Business Management, Department of Forest Resources Utilization, Korean Forest Research Institute, Seoul 130-712, South Korea

ARTICLE INFO

Article history:
Received 19 January 2012
Revised 3 April 2012
Accepted 16 April 2012
Available online 24 April 2012

Keywords:
Celtis biondii
Ethyl 2,4,6-trihydroxybenzoate
Liver X receptor
Cholesterol

ABSTRACT

The present study reports a novel liver X receptor (LXR) activator, ethyl 2,4,6-trihydroxybenzoate (ETB), isolated from *Celtis biondii*. Using a reporter gene assay, time-resolved fluorescence resonance energy transfer (TR-FRET), and surface plasmon resonance (SPR) analysis, we showed that ETB directly bound to and stimulated the transcriptional activity of LXR-α and LXR-β. In macrophages, hepatocytes, and intestinal cells, ETB suppressed cellular cholesterol accumulation in a dose-dependent manner and induced the transcriptional activation of LXR-α/-β-responsive genes. Notably, ETB did not induce lipogenic gene expression or cellular triglyceride accumulation in hepatocytes. These results suggest that ETB is a dual-LXR modulator that regulates the expression of key genes in cholesterol homeostasis in multiple cells without inducing lipid accumulation in HepG2 cells.

Atherosclerosis is the leading cause of death worldwide, accounting for approximately 72 million deaths each year.[1] Epidemiological studies have identified high levels of low-density lipoprotein (LDL) cholesterol and reduced levels of high-density lipoprotein (HDL) cholesterol as major contributors to atherogenesis.[2] Accordingly, HDL-raising therapies have generated interest. It was recently demonstrated that nuclear receptor LXRs regulate the cholesterol and phospholipid pump by activating the transcription of ATP-binding cassette (ABC) A1/G1/G5/G8 and apolipoprotein E (apoE). Thus, LXR agonists are potential HDL-raising agents that could act on the artery wall to stimulate the efflux of cholesterol from lipid-laden macrophages. Treatment of atherosclerotic mice with synthetic LXR ligands, such as GW3965 and T0901317, inhibit progression and promote regression of atherosclerotic plaques. Furthermore, transplantation of macrophages lacking LXR-α/-β into a host that is predisposed to atherogenesis results in increased foam cell differentiation and arterial plaque formation, even after treatment with LXR agonists.[3,4]

These results highlight the cardioprotective roles of LXRs. However, studies have also shown that LXR agonists can cause liver steatosis and increase serum triglyceride levels in rodents by activating hepatic SREBP-1c.[5,6] Thus, specific LXR ligands that do not induce fatty acid synthesis in the liver are of interest. Several groups have described agents that have beneficial effects on lipid metabolism. Vlasuk et al.[7] and Kratzer and co-workers[8] identified two novel LXR agonists, WAY-252623 and *N,N*-dimethyl-3β-hydroxy-cholenamide, that reduce atherosclerosis without activating SREBP1c or increasing hepatic lipogenesis. This raised the possibility that some of the anti-atherosclerotic effects of LXR agonists may be independent of systemic lipid metabolism in hepatocytes and may be attributable to direct actions on the vascular wall that activate reverse cholesterol transport (RCT). Hence, LXR is an attractive target for novel pharmaceutical agents.

Plant medicines have become increasingly popular for the prevention and/or treatment of cardiovascular disease and have proven to be an abundant source of pharmacological agents for medicinal purposes. The characterization of key active compounds is essential.[9] Initially, we screened approximately 900 Korean medicinal plant and lipidarine extracts for LXR agonist activity and found that *Celtis biondii* (*CB*) ethanol extract had potent LXR agonist activity. In this study, we isolated an LXR agonistic

Abbreviations: ABC, ATP-binding cassette transporter; FAS, fatty acid synthase; HDL, high-density lipoprotein; LBD, ligand-binding domain; LDL, low-density lipoprotein; LXR, liver X receptor; NPC1L1, Niemann-Pick C1 Like 1; SCD-1, stearoyl-CoA desaturase 1; SPR, surface plasmon resonance; SREBP, sterol regulatory element-binding protein; TG, triglyceride; TR-FRET, timeresolved fluorescence resonance energy transfer.

* Corresponding author. Tel./fax: +82 2 3290 3494.
E-mail address: junelee@korea.ac.kr (S.-J. Lee).

0960-894X/$ - see front matter © 2012 Elsevier Ltd. All rights reserved.
http://dx.doi.org/10.1016/j.bmcl.2012.04.071

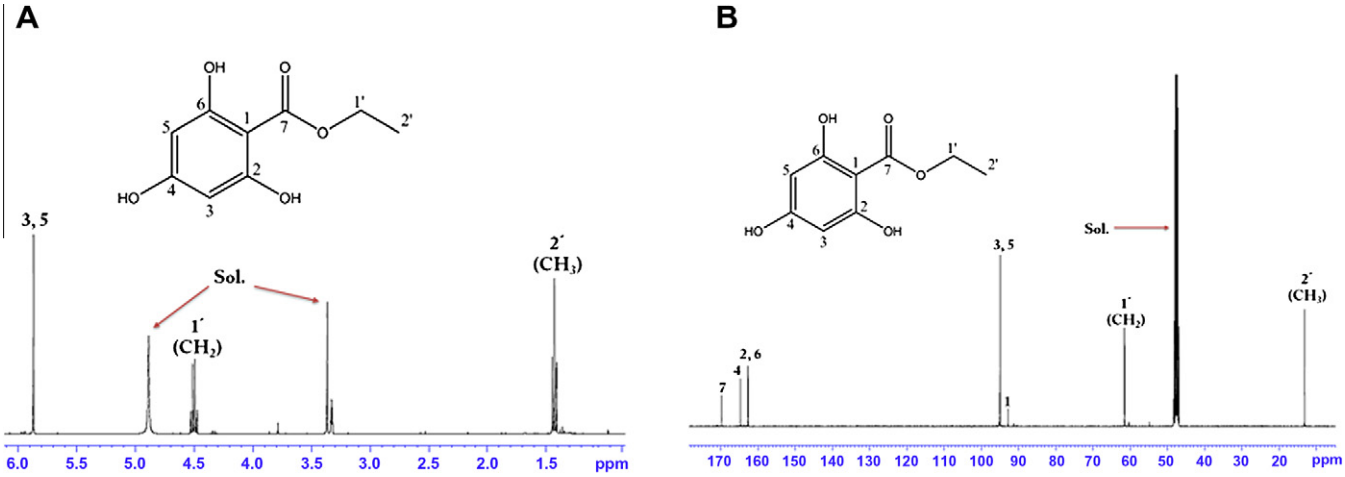

Figure 1. ^{1}H NMR (A) and ^{13}C NMR (B) spectra for ETB.

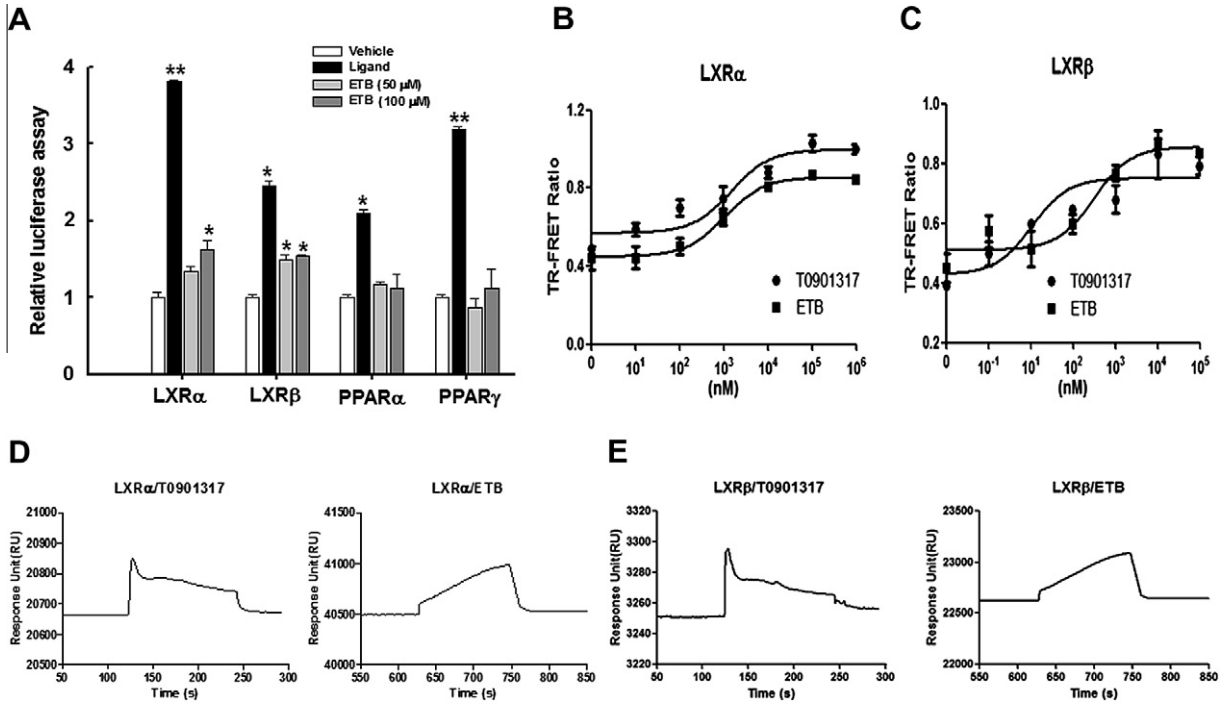

Figure 2. ETB activates LXR-α and LXR-β by directly interacting with their ligand-binding domains. (A) ETB activates LXR-α and LXR-β but not PPAR-α and PPAR-γ transactivation activity. HEK 293 cells were transfected with expression plasmids for receptors and a pSV-β-galactosidase together with a reporter plasmid (pGL4.35[luc2P/9XGAL4UAS/Hygro] for LXRs and pCMV-3xPPRE-Luc for PPARs). The cells were exposed to ETB (50 and 100 μM), receptor-specific ligands (1 μM T0901317 for LXRs, 10 μM fenofibric acid for PPAR-α, and 10 μM troglitazone for PPAR-γ), or vehicle control (1% DMSO) for 24 h before assaying luciferase activity. Activation of LXR-α (B) and LXR-β (C) by T0901317 and ETB as assessed by TR-FRET assay. The direct interactions between ETB (100 μM) or T0901317 (1 μM) and the immobilized LXR-α-LBD (D) and LXR-β-LBD (E) were examined by SPR on a Biacore instrument. Data represent the mean ± SE; $^{*}P$ <0.05 versus control (n = 8).

compound from *CB* ethanol extract and investigated its metabolic effect on lipid metabolism.

Lyophilized *CB* root powder was extracted with EtOH at room temperature for 72 h. The EtOH extract (81.23 g) was partitioned into two subfractions using organic solvents, yielding *n*-hexane-soluble (4.26 g) and CH_2Cl_2-soluble (4.14 g). The CH_2Cl_2 fraction was further subjected to multiple chromatographic steps on a Sephadex LH-20 column (6.0 × 47.0 cm) to provide the compound CBD-III (Supplementary Fig. 1).

Next, the structure of this compound was elucidated using MS, ^{1}H, and ^{13}C NMR spectra analysis[10] and by direct comparison with published data.[11] The compound produced a molecular ion peak at 188 $[M]^{+}$ in the EI-MS spectrum. The ^{1}H NMR spectrum showed ethyl signals at δ 1.43 (3H, t, H-2′) and δ 4.50 (2H, *dd*, H-1′) and an aromatic proton signal at δ 5.87 (2H, *s*, H-3, H-5). The low-field shift of the methylene group was suggestive of an ester group (Fig. 1A). In the ^{13}C NMR spectrum, there were two ethyl group signals [δ 13.22 (*q*, C-2′) and δ 61.59 (*t*, C-1′)], four aromatic signals [δ 92.86 (*s*, C-1), 162.66 (*s*, C-2, C-6), 164.73 (*s*, C-4)], and an ester carbonyl signal [δ 169.76 (*s*, C-7)]. Among the aromatic C signals, the chemical shifts at δ 95.00 (*d*, C-3, C-5) and δ 92.86 (*s*, C-1) were attributable to the C–H and C–C groups, respectively, and the remaining signals at δ 164.73 (*s*, C-4) and δ 162.66 (*s*, C-2, C-6) were attributable to a C–O group, indicative of a methyl 2,4,6-trihydroxybenzoate moiety (Fig. 1B).[11] Based on these data, the compound was identified as ethyl 2,4,6-trihydroxybenzoate (ETB).

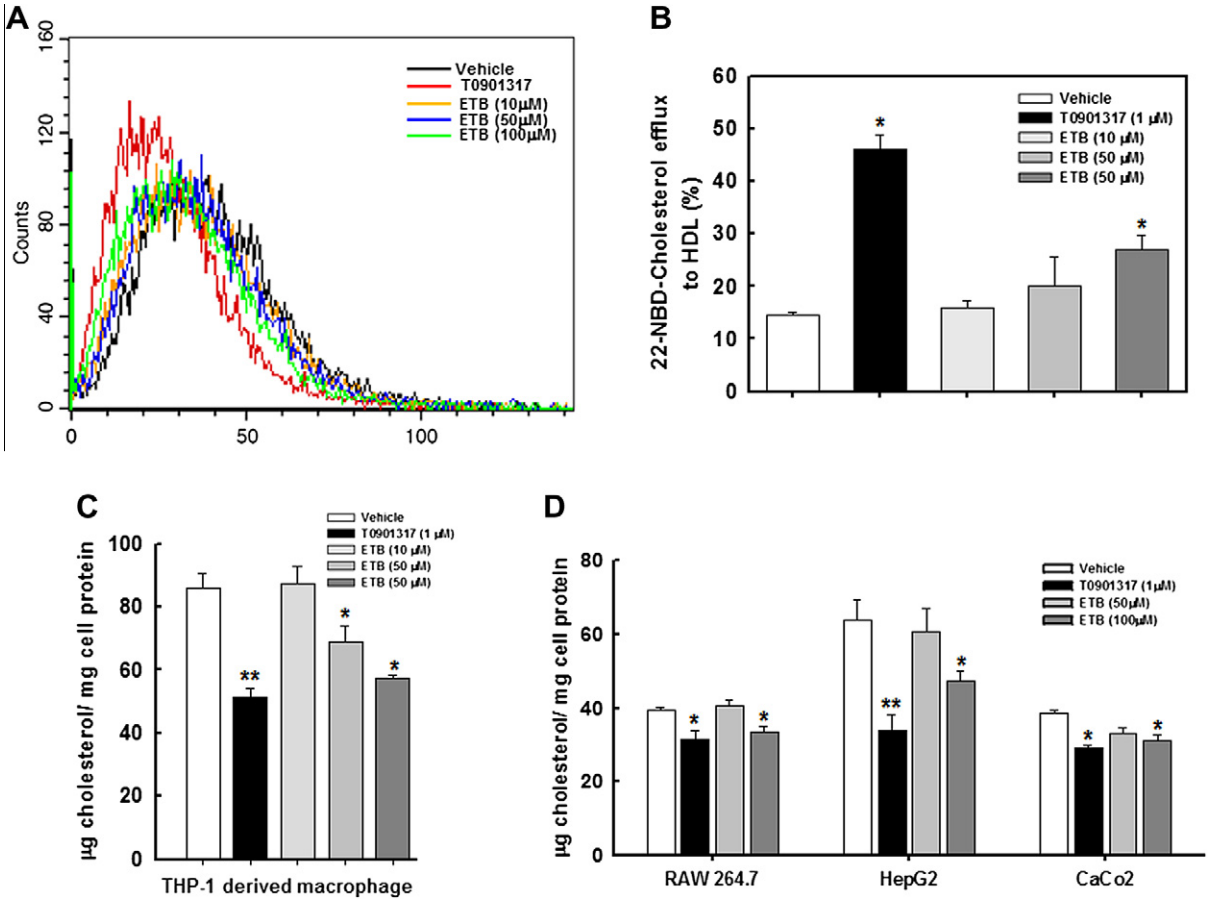

Figure 3. ETB induces cholesterol efflux in THP-1-derived macrophages and reduces intracellular cholesterol levels in multiple cell types. (A) and (B) Cholesterol efflux was quantified using 22-NBD-cholesterol and FACS analysis.[15] (A) FACS profile of cholesterol efflux to HDL in THP-1-derived macrophages. (B) Relative 22-NBD-cholesterol efflux to HDL. (C) Intracellular cholesterol concentrations in THP-1-derived macrophages. (D) Intracellular cholesterol concentrations in RAW 264.7 macrophages, HepG2, and Caco2. Data represent the mean ± SE; $^{*}P$ <0.05 and $^{**}P$ <0.01 versus control (n = 3–5).

Cell viability was measured using the MTT [3-(4,5-dimethylthiazole-2-yl)-2,5-diphenyltetrazolium bromide] colorimetric method.[19] ETB did not affect cell viability in THP-1-derived macrophages, RAW 264.7 macrophages, and HepG2 cells at various concentrations (Supplementary Fig. 2). The reporter gene assay was performed in cultured HEK 293 cells[12] to measure the transactivation of LXR-α and -β. HEK 293 cells were co-transfected with the pGL4.35[luc2P/9XGAL4UAS/Hygro] vector and either pFN26AhLXRα or pFN26Ah LXRβ, and then incubated with ETB, T0901317 (positive control), or a vehicle (1% DMSO). ETB incubation significantly induced the transactivation of both LXR-α (+64% at 100 μM; P <0.05) and LXR-β (+55% at 100 μM; P <0.05) in a dose-dependent fashion (Fig. 2A), and the EC_{50} of ETB was 80.76 and 37.8 μM for LXR-α and -β, respectively. Similarly, T0901317 (a synthetic ligand of LXRs) showed significant activation of both isoforms compared to that of the vehicle. ETB did not affect transactivation of PPAR-α or PPAR-γ, whereas transactivation activity of PPAR-α and PPAR-γ was induced by the positive control fenofibrate and GW0742 (Fig. 2A).

ETB could modulate LXR activity directly (by interacting with the ligand-binding domains [LBDs] of LXRs) or indirectly (by inducing the synthesis of an endogenous ligand). To confirm the direct binding of ETB to LXR-LBD proteins, TR-FRET and SPR assays were performed as described previously.[13] First, the TR-FRET assay results showed that the synthetic LXR ligand T0901317, by binding specifically to LXR-α and LXR-β, strongly enhanced the recruitment of Trap 220/Drip-2 and D22 coactivator peptide, respectively, with EC_{50} values of 1.43 μM (LXR-α) and 0.11 μM (LXR-β) (Fig. 2B and C). Similarly, ETB induced the recruitment of Trap 220/Drip-2 coactivator peptide to LXR-α-LBD and D22 co-activator peptide to LXR-β-LBD in a dose-dependent manner. ETB showed strong ligand binding and coactivator recruitment for both LXRs using a cell-free FRET assay with estimated EC_{50} values of 1.50 and 3.04 μM for LXR-α and LXR-β, respectively. However, this compound did not activate LXRs in a cell-based reporter gene assay at similar concentrations. In the reporter gene assay, the EC_{50} of ETB was 80.76 and 37.8 μM for LXR-α and -β, respectively. The reason for this remains unknown; however, it is possible that ETB may not be taken into the cells and has a low bioavailability.

Second, T0901317 and ETB were analyzed with the SPR-Biacore system to assess the direct interaction between LXRs–LBD proteins and ETB. ETB was directly associated with two LXR subtypes (Fig. 2D and E). Our results demonstrate that ETB activates the nuclear receptors LXR-α and LXR-β by binding directly to the LBD of the receptors, and could thereby stimulate target gene transcription for cholesterol homeostasis in macrophages, hepatocytes, and intestinal cells.

The activation of LXR-α promotes cholesterol efflux, stimulates RCT in macrophages, and inhibits the accumulation of cholesterol in vitro and in vivo.[14] Therefore, we next investigated the effect of ETB treatment on cholesterol efflux in THP-1-derived macrophages[15] and cellular cholesterol content in multiple cell types.[16] ETB increased cholesterol efflux to HDL (Fig. 3A) and reduced cellular cholesterol concentration in a dose-dependent manner in THP-1-derived macrophages (Fig. 3B). These effects of ETB were significant compared to the control at concentrations of 50 and 100 μM. T0901317 showed similar results, in agreement with a

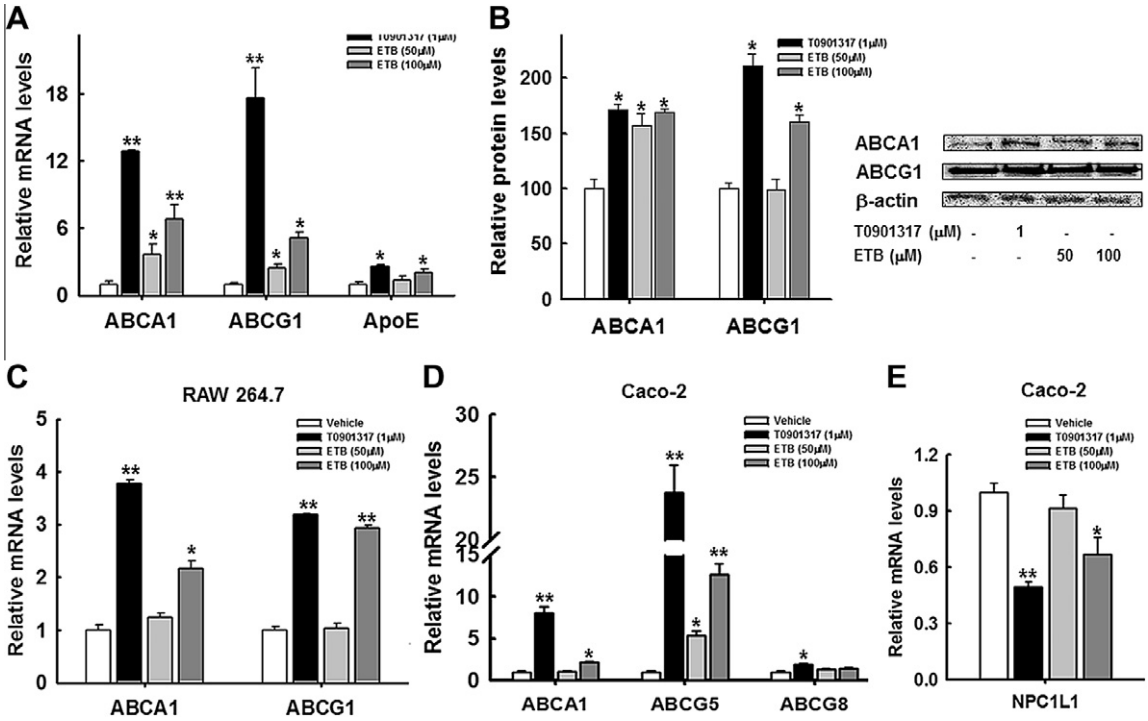

Figure 4. ETB-induced changes in gene and protein expression in macrophages and Caco2 cells. THP-1 monocytes were incubated with PMA (50 ng/mL) for 3 days to differentiate them into adherent macrophages. Then the macrophages and Caco2 cells were treated with 50 and 100 μM ETB, 1 μM T0901317, or vehicle control (1% DMSO) for 48 h. Total RNA was extracted and mRNA expression levels of ABCA1, ABCG1, and APOE in THP-1-derived macrophages (A), ABCA1 and ABCG1 in RAW 264.7 (C), and ABCA1, ABCG1, ABCG5, and NPC1L1 in Caco2 (D, E) were measured by qPCR.[23] The protein levels of ABCA1 and ABCG1 in THP-1-derived macrophages were determined by immunoblotting (B).[24] Data are shown as the mean ± SEM ($n = 3$). *, ** Significantly different gene expression compared to the control group, $^{*}P < 0.05$, $^{**}P < 0.001$.

previous study by Aravindhan et al.[17] Interestingly, ETB reduced cholesterol levels in RAW 264.7 macrophages, HepG2, and intestinal cells in a dose-dependent manner. At an ETB concentration of 100 μM, the reduction relative to the positive control was statistically significant (Fig. 3C). Thus, we used two concentrations (50 and 100 μM) for further experiments. These concentrations are rather high, but not unusual for in vitro experiments using gallate and its derivatives.[18]

Numerous LXR target genes are involved in the reverse cholesterol transport pathway in macrophages.[14] Intracellular accumulation of cholesterol in macrophages leads to increased expression of ABCA1, which facilitates the transport of excess macrophage cholesterol to extracellular acceptors (such as apoAI and HDL) for subsequent transport as HDL particles to the liver. Considerable evidence has established that LXRs are critical regulators of the ABCA1-dependent cholesterol efflux pathway.[20] In addition, another cholesterol efflux transporter, ABCG1, is induced in macrophages in response to LXR ligands.[21] ApoE is also an LXR target gene involved in cholesterol homeostasis, and mice lacking ApoE spontaneously develop atherosclerosis.[22] Therefore, we performed quantitative PCR (qPCR) and immunoblotting analysis of LXR target genes and protein, respectively.[23,24] ETB significantly and dose-dependently increased the expression of LXR-responsive genes ABCA1 and ABCG1 in macrophages (Fig. 4A and C). At a concentration of 100 μM, ETB increased ABCA1 mRNA expression 7.4-fold ($P < 0.01$) for THP-1-derived macrophages (Fig. 4A) and 2.1-fold ($P < 0.05$) for RAW 264.7 macrophages (Fig. 4C), respectively, compared to the control group. ABCG1 mRNA levels increased 5.2- and 2.9-fold after THP-1-derived macrophages and RAW 264.7 cells were treated with 100 μM ETB, respectively (Fig. 4A and C). Immunoblot analysis showed results similar to those of the qPCR analysis in THP-1-derived macrophages (Fig. 4B). ApoE increased 1.9-fold after treatment of THP-1-derived macrophage with 100 μM ETB (Fig. 4A). A greater effect was observed in cells stimulated with T0901317. The effects of ETB in macrophage cells were similar to those of LXR-α and LXR-β agonists, which increase cholesterol efflux by inducing ABCA1, ABCG1, and ApoE. Together, these findings suggest that as an LXR ligand, ETB suppresses cholesterol accumulation by promoting an efflux pathway in macrophages, which could elevate circulating levels of HDL-cholesterol and prevent hypercholesterolemia and atherosclerosis.

LXR also impacts systemic cholesterol levels by decreasing intestinal cholesterol absorption and increasing biliary cholesterol excretion via the regulation of NPC1L1 and the transporters ABCA1, ABCG5, and ABCG8.[14,25] In Caco2 cells, intestinal ABCA1, ABCG5, and ABCG8 mRNA levels increased 2.1-, 12.6-, and 1.5-fold, respectively, after stimulation with 100 μM ETB (Fig. 4D). Compared to the controls, the expression of NPC1L1 mRNA was significantly reduced by 33.2% in Caco-2 cells stimulated with 100 μM ETB. Reduction of intestinal cholesterol uptake by ETB may provide additional benefits to prevent hypercholesterolemia and atherosclerosis.

The role of LXR in the control of fatty acid metabolism has been implicated as a potential side effect of LXR therapy. The expression of fatty acid synthesis genes including sterol regulatory element-binding protein-1c (SREBP-1c), fatty acid synthase (FAS), and stearoyl-CoA desaturase-1 (SCD-1) is blunted in mice carrying a targeted disruption in the LXR-α gene.[26] On the other hand, administration of synthetic LXR ligands to mice elevates plasma triglyceride levels in part by inducing the hepatic lipogenic pathway.[6] In this study, stimulation of HepG2 cells with T0901317 increased cellular TG levels, as previously reported (Fig. 5A and B), and also induced the expression of SREBP-1c, FAS, and SCD-1 (Fig. 5C). However, ETB did not increase cellular TG concentrations in hepatocytes, as assessed by direct measurement as well as DiI and Oil Red O-lipid staining (Fig. 5A and B).[27] In contrast, T0901317-treated cells showed significant accumulation of cellular lipid droplets (Fig. 5B). Compared to vehicle-treated control cells, treatment with ETB at 50 and 100 μM reduced SCD-1 mRNA levels by 47.6%, and 54.9%, respectively, and

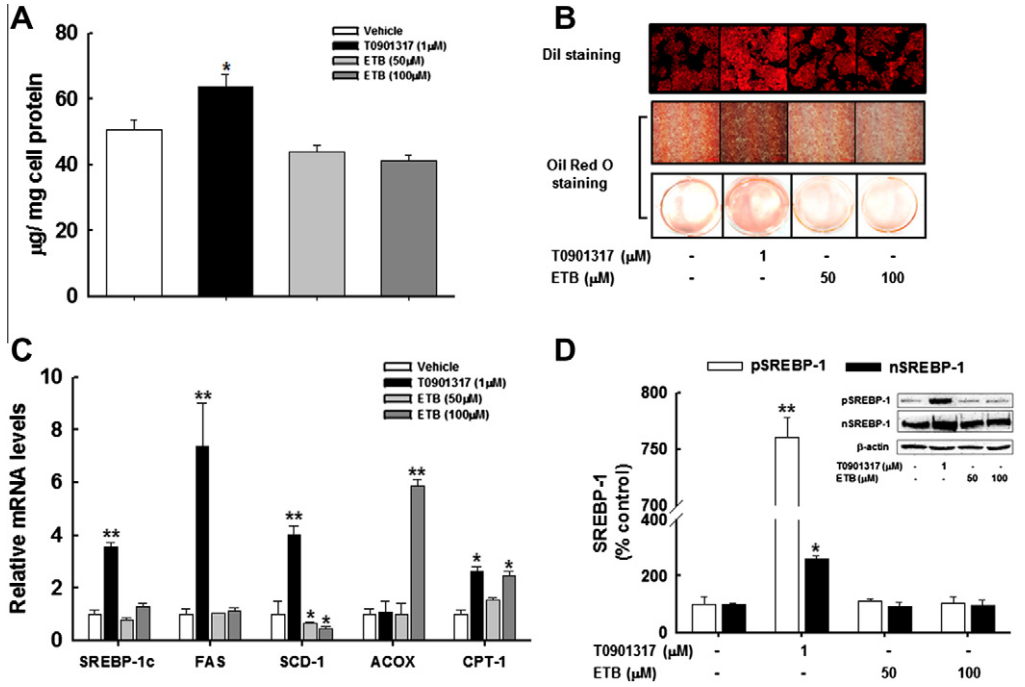

Figure 5. ETB has modest effects on intracellular triglyceride levels in HepG2 cells and the expression of hepatic lipogenesis genes and proteins. (A) Intracellular triglyceride levels in HepG2 cells. (B) Lipid staining of HepG2 incubated with ETB and T0901317[27] shows fat accumulation in cells stained with DiI or Oil Red O. (C) Expression of the genes encoding SREBP-1c, FAS, SCD-1, CPT-1, and ACOX in HepG2 cells incubated with ETB and T0901317, as assessed by qPCR. Results are normalized to the GAPDH or cyclophilin mRNA levels. (D) The protein expression levels of SREBP-1 in HepG2 cells were determined by immunoblotting with anti-SREBP-1.[24] Data represent the mean ± SE; $^{*}P$ <0.05 and $^{**}P$ <0.01 versus control (n = 3–5).

did not affect the expression of SREBP-1c or FAS (Fig. 5C). We further assessed the protein expression of SREBP-1, a key transcription factor of FAS and SCD-1, to investigate the regulatory mechanism of ETB in lipid metabolism in HepG2 cells.[24] ETB did not affect the precursor or nuclear form of SREBP-1 whereas protein expression was significantly induced by T0901317 (Fig. 5D).

The mechanisms of ETB upregulation of FAS and SCD-1 are currently unclear. However, differential co-activator and corepressor recruitment is a determinant of nuclear receptor tissue specificity[28] and may play a role in ETB activity. Miao et al.[29] and Albers et al.[30] reported that the selective LXR modulators GW3965 and 22R-HC differ in their induction of FAS and SCD-1 in the liver (compared to T0901317) due to differences in the extent of co-activator recruitment. For LXR-α, coactivators such as SRC-1 and DRIP are recruited in similar amounts by T0901317 and GW3965. In contrast, GW3965 recruits less CBP than T0901317. It is tempting to speculate that SRC-1 and DRIP mediate the intestinal effects on gene expression, while other coactivators such as CBP mediate the effects of these two ligands on the liver after they bind LXR-α. In the present study, ETB was less effective at recruiting TRAP220/DRIP-2 to LXR-α than T0901317. Hence, it is possible that other coactivators besides the ones we tested may mediate the tissue-selective differences of T0901217 and ETB.

Musso et al.[31] reported that reduced lipogenesis by SCD-1 inhibition is related to enhanced hepatic fatty acid oxidation via increased carnitine palmitoyltransferase 1 (CPT-1). Because ETB did not affect cellular TG content or SCD-1 expression in HepG2 cells, we further investigated the effect of ETB treatment on mRNA expression of fatty acid oxidation genes in HepG2 cells.[23] Stimulation of HepG2 cells with ETB at a concentration of 100 μM significantly induced the expression of CPT-1 and ACOX (key genes in fatty acid oxidation) compared to controls (Fig. 5C). Strong antioxidative potential of trihydroxybenzoate may affect hepatic fatty acid oxidation.[32] Taken together, these findings suggest that ETB induces fatty acid oxidation gene expression, but does not affect the expression of the lipogenic gene SCD-1 in hepatocytes.

In conclusion, we isolated ETB from *C. biondii* and demonstrated that it exhibits LXR agonist activity. We showed that ETB is a direct ligand of LXR-α and LXR-β and that it stimulates cholesterol efflux in macrophages without hepatic lipid accumulation. The findings of the present study provide insight that may be useful in the development of pharmaceutical agents for treating hypercholesterolemia and atherosclerosis.

Acknowledgments

We appreciate the technical assistance of Hea-Won Kim. This study was supported by the Korean Forest Service (Forest Science & Technology Project No. S120909L130110), by the Technology Development Program for Fisheries of the Ministry for Food, Agriculture, Forestry and Fisheries, Republic of Korea (iPET, F20926409H220000110), and by the Basic Science Research Program through the National Research Foundation of Korea (NRF) funded by the Ministry of Education, Science and Technology (20100028180), and by a Korea University Grant.

Supplementary data

Supplementary data associated with this article can be found, in the online version, at http://dx.doi.org/10.1016/j.bmcl.2012.04.071.

References and notes

1. Murray, C. J.; Lopez, A. D. *Science* **1996**, *274*, 740.
2. Lusis, A. J. *Nature* **2000**, *407*, 233.
3. Joseph, S. B.; McKilligin, E.; Pei, L.; Watson, M. A.; Collins, A. R.; Laffitte, B. A.; Chen, M.; Noh, G.; Goodman, J.; Hagger, G. N.; Tran, J.; Tippin, T. K.; Wang, X.; Lusis, A. J.; Hsueh, W. A.; Law, R. E.; Collins, J. L.; Willson, T. M.; Tontonoz, P. *Proc. Natl. Acad. Sci. U.S.A.* **2002**, *99*, 7604.

4. Levin, N.; Bischoff, E. D.; Daige, C. L.; Thomas, D.; Vu, C. T.; Heyman, R. A.; Tangirala, R. K.; Schulman, I. G. *Arterioscler. Thromb. Vasc. Biol.* **2005**, *25*, 135.
5. Chisholm, J. W.; Hong, J.; Mills, S. A.; Lawn, R. M. *J. Lipid Res.* **2003**, *44*, 2039.
6. Schultz, J. R.; Tu, H.; Luk, A.; Repa, J. J.; Medina, J. C.; Li, L.; Schwendner, S.; Wang, S.; Thoolen, M.; Mangelsdorf, D. J.; Lustig, K. D.; Shan, B. *Gene Dev.* **2000**, *14*, 2831.
7. Vlasuk, G. P.; Quinet, E. M.; Basso, M. D.; Halpern, A. R.; Yates, D. W.; Steffan, R. J.; Clerin, V.; Resmini, C.; Keith, J. C.; Berrodin, T. J.; Feingold, I.; Zhong, W. Y.; Hartman, H. B.; Evans, M. J.; Gardell, S. J.; DiBlasio-Smith, E.; Mounts, W. M.; LaVallie, E. R.; Wrobel, J.; Nambi, P. *J. Lipid Res.* **2009**, *50*, 2358–2370.
8. Kratky, D.; Kratzer, A.; Buchebner, M.; Pfeifer, T.; Becker, T. M.; Uray, G.; Miyazaki, M.; Miyazaki-Anzai, S.; Ebner, B.; Chandak, P. G.; Kadam, R. S.; Calayir, E.; Rathke, N.; Ahammer, H.; Radovic, B.; Trauner, M.; Hoefler, G.; Kompella, U. B.; Fauler, G.; Levi, M.; Levak-Frank, S.; Kostner, G. M. *J. Lipid Res.* **2009**, *50*, 312.
9. Bramlett, K. S.; Houck, K. A.; Borchert, K. M.; Dowless, M. S.; Kulanthaivel, P.; Zhang, Y.; Beyer, T. P.; Schmidt, R.; Thomas, J. S.; Michael, L. F.; Barr, R.; Montrose, C.; Eacho, P. I.; Cao, G.; Burris, T. P. *J. Pharmacol. Exp. Ther.* **2003**, *307*, 291.
10. NMR experiments were performed using a Varian UI 500 spectrometer (Varian, Inc., Palo Alto, CA, USA) at operating frequencies of 400 MHz (^{1}H) and 100 MHz (^{13}C) at the Korea Basic Science Institute in Seoul. EI-MS: JEOL JMS-600W, direct inlet at 70 eV. In all experiments, MeOH-d_4 was used as an internal standard.
11. Lee, Y. R.; Wang, X. *Bull. Korean Chem. Soc.* **2007**, *28*, 2061.
12. HEK 293, murine macrophage-like RAW 264.7, human monocytic THP-1, Caco2, and HepG2 cells were obtained from the Korean Cell Line Bank (Seoul, Korea). HEK 293, RAW 264.7, and HepG2 were cultured in Dulbecco's minimum essential medium (DMEM) supplemented with 10% FBS and 1% penicillin/streptomycin (PES) before treatment. Human monocytic THP-1 cells were maintained in RPMI-1640 medium supplemented with 10% FBS, 0.05 mM β-mercaptoethanol, and 1% PES. Caco2 cells were maintained in MEM medium supplemented with 20% FBS and 1% PES. All cell lines were grown in 5% CO2 at 37 °C. Prior to the experiments, THP-1 cells were differentiated in the presence of 50 ng/mL PMA for 72 h. RAW 264.7 macrophages, Caco2, and HepG2 cells were preincubated in serum-free medium for 24 h. The following day, the medium was removed and the cells were incubated for an additional 48 h in 2 mL medium containing 1 μM T0901317 (positive control), ETB (50 or 100 μM), or vehicle (1% DMSO).
13. Jia, Y.; Bhuiyan, M. J. H.; Jun, H. J.; Lee, J. H.; Hoang, M. H.; Lee, H. J.; Kim, N.; Lee, D.; Hwang, K. Y.; Hwang, B. Y.; Choi, D. W.; Lee, S. J. *Bioorg. Med. Chem. Lett.* **2011**, *21*, 5876.
14. Geyeregger, R.; Zeyda, M.; Stulnig, T. M. *Cell. Mol. Life Sci.* **2006**, *63*, 524.
15. THP-1 cells were plated in 6-well plates at a density of approximately 106 cells/well and differentiated in the presence of 50 ng/mL PMA for 72 h. The following day, the medium was removed and the cells were incubated for an additional 48 h in 2 mL medium containing 1 μM T0901317 (positive control), ETB (50 or 100 μM), or vehicle (1% DMSO). Then they were loaded with 1.5 μM 22-NBD-cholesterol (Invitrogen) in medium containing 2.5% FBS for 1 h in a 37 °C CO_2 incubator. After loading, the cells were washed twice with Puck′s buffer (1 mM Na_2HPO_4, 0.9 mM H_2PO_4, 5.0 mM KCl, 1.8 mM $CaCl_2$, 0.6 mM $MgSO_4$, 6 mM glucose, 138 mM NaCl, and 10 mM HEPES) and placed in serum-free medium. HDL (10 μg/mL) was added to start the efflux experiment. After 4 h incubation, the medium was removed and cells were resuspended in FACS buffer and analyzed using flow cytometry (FACS Calibur; BD Biosciences, San Jose, CA, USA) by determining FL-1 fluorescence 25. The data were analyzed using Cell Quest Pro software (BD Biosciences). The HDL-dependent efflux of 22-NBD-cholesterol was calculated as follows for each condition: percentage of (22-NBD-cholesterol in cells in medium without HDL) − (22-NBD-cholesterol in cells in medium with HDL). Each efflux assay was performed in triplicate.
16. Cells were washed with ice-cold PBS and cellular lipids were extracted at room temperature with 2 mL of a 2:1 (v:v) mixture of hexane and isopropanol. The organic solvent was removed by vacuum centrifugation and the lipids were resuspended in 200 μL 95% ethanol. TG and cholesterol concentrations were enzymatically determined using the Cobas C111 analyzer and an Amplex Red Cholesterol Assay Kit (Invitrogen), respectively, according to the manufacturer's instructions. The concentrations were normalized to total protein concentrations.
17. Aravindhan, K.; Webb, C. L.; Jaye, M.; Ghosh, A.; Willette, R. N.; DiNardo, N. J.; Jucker, B. M. *J. Lipid Res.* **2006**, *47*, 1250.
18. Pajak, B.; Kania, E.; Gajkowska, B.; Orzechowski, A. *J. Physiol. Pharmacol.* **2011**, *62*, 449.
19. The viability of cultured cells was determined based by the amount of MTT reduced to formazan. After treatment with various concentrations of ETB (1, 5, 10, 50, 100, and 200 M) or 1% of DMSO as a vehicle control, culture medium containing MTT (0.5 mg/mL) was added to each well and the cells were incubated at 37 °C for 3 h before mixing with DMSO to dissolve the formazan crystals. Then the absorbance at 570 nm was measured. Values were normalized to the sample protein concentrations.
20. Costet, P.; Luo, Y.; Wang, N.; Tall, A. R. *J. Biol. Chem.* **2000**, *275*, 28240.
21. Schmitz, G.; Langmann, T.; Heimerl, S. *J. Lipid Res.* **2001**, *42*, 1513.
22. Laffitte, B. A.; Repa, J. J.; Joseph, S. B.; Wilpitz, D. C.; Kast, H. R.; Mangelsdorf, D. J.; Tontonoz, P. *Proc. Natl. Acad. Sci. U.S.A.* **2001**, *98*, 507.
23. Total RNA was extracted from THP-1, RAW 264.7, HepG2, and Caco2 cells using TRIzol reagent according to the manufacturer's instructions. cDNA was synthesized from 2 μg total RNA using Superscript II reverse transcriptase (Invitrogen) and oligo(dT) primers. Gene expression was measured using an iQ5 Real Time PCR Detection System (Bio-Rad) and Bio-Rad iQ SYBR Green Supermix reagent. The reaction conditions were 95 °C for 3 min, followed by 50 cycles of 95 °C for 10 s, 57 °C for 15 s, and 72 °C for 20 s. A melting curve was performed for 71 cycles starting at 45 °C and increased by 0.5 °C every 10 s. Relative levels of gene expression were calculated using iQ5 Optical System Software version 2 (Bio-Rad), with the expression of each target gene being normalized to that of cyclophillin or glyceraldehyde 3-phosphate dehydrogenase (GAPDH). The primer sequences are shown in Supplementary Table 1.
24. THP-1 and HepG2 cells were lysed in ice-cold lysis buffer containing 10 mM Tris–HCl (pH 7.4), 0.1 M EDTA, 10 mM NaCl, 0.5% Triton X-100, and protease inhibitor cocktail (Roche, Mannheim, Germany). The lysate was clarified by centrifugation at 14,000 rpm for 10 min at 4 °C. To quantify SREBP-1, proteins were isolated from the nuclear and membrane fractions using a nuclear extraction kit (Cayman Chemical, Ann Arbor, MI, USA) according to the manufacturer's protocol. Sample protein content was determined using a BCA Protein Assay kit (Pierce). Protein samples (30 μg) were subjected to 10% SDS–PAGE and then transferred to and immobilized on nitrocellulose membranes. After blocking, the membranes were probed with primary antibody (anti-SREBP-1, anti-ABC1, anti-ABCG1, anti-actin; Santa Cruz Biotechnology) and then incubated with secondary antibody (anti-rabbit IgG-HRP or anti-mouse IgG-HRP; Santa Cruz Biotechnology). Immunoreactive bands were imaged with a ChemiDoc XRS imaging system (Bio-Rad) using PowerOpti-ECL Western blotting detection reagent (Anigen). The relative band intensities were determined using Gel-Pro Analyzer 4.0 software (Media Cybernetics). For each sample, target protein levels were normalized to β-actin (internal reference).
25. Tang, W. Q.; Ma, Y. Y.; Jia, L.; Ioannou, Y. A.; Davies, J. P.; Yu, L. Q. *Arterioscler. Thromb. Vasc. Biol.* **2008**, *28*, 448.
26. Peet, D. J.; Turley, S. D.; Ma, W.; Janowski, B. A.; Lobaccaro, J. M.; Hammer, R. E.; Mangelsdorf, D. J. *Cell* **1998**, *93*, 693.
27. HepG2 cells were labeled with the Vybrant DiI cell labeling solution (Molecular Probes, Carlsbad, CA, USA) in accordance with the manufacturer′s instructions. For Oil Red O staining, cells were washed with PBS and fixed through incubation in 10% (v:v) formalin at room temperature for 1 h. The cells were stained with Oil Red O (in 60% v:v isopropanol) for 15 min and rinsed thoroughly with distilled water. Stained lipid droplets were visualized using an Eclipse Ti inverted microscope (Nikon). Lipid accumulation was quantified through isopropanol extraction of Oil Red O from stained cells and optical density determinations at 500 nm using a SmartSpec Plus spectrophotometer (Bio-Rad).
28. Stafslien, D. K.; Vedvik, K. L.; De Rosier, T.; Ozers, M. S. *Mol. Cell. Endocrinol.* **2007**, *264*, 82.
29. Miao, B.; Zondlo, S.; Gibbs, S.; Cromley, D.; Hosagrahara, V. P.; Kirchgessner, T. G.; Billheimer, J.; Mukherjee, R. *J. Lipid Res.* **2004**, *45*, 1410.
30. Albers, M.; Blume, B.; Schlueter, T.; Wright, M. B.; Kober, I.; Kremoser, C.; Deuschle, U.; Koegl, M. *J. Biol. Chem.* **2006**, *281*, 4920.
31. Musso, G.; Gambino, R.; Cassader, M. *Prog. Lipid Res.* **2009**, *48*, 1.
32. RamisRamos, G. *ANTIOXIDANTS–Synthetic Antioxidants*; Academic Press, 2003.